Supporting Information

Terminal Deuterium Atoms Protect Silicon from Oxidation

Tiexin Li [a], Chandramalika R. Peiris [a], Albert C. Aragonès [b,c], Carlos Hurtado [a], Anthony Kicic[d,e,f,g], Simone Ciampi [a], Melanie MacGregor [h], Tamim Darwish [i], Nadim Darwish [a]*

[a] School of Molecular and Life Sciences, Curtin University, Bentley, WA 6102, Australia

[b] Departament de Ciència de Materials i Química Física, Universitat de Barcelona, Marti i Franquès 1, 08028 Barcelona, Spain

[c] Institut de Química Teòrica i Computacional (IQTC), Universitat de Barcelona, Diagonal 645, 08028 Barcelona, Spain

[d] Occupation, Environment and Safety, School of Population Health, Curtin University, Perth, WA, 6845, Australia

[e] Wal-Yan Respiratory Research Centre, Telethon Kids Institute, The University of Western Australia, Nedlands, WA, 6009, Australia

[f] Department of Respiratory and Sleep Medicine, Perth Children's Hospital, Nedlands, WA, 6009, Australia

[g] Centre for Cell Therapy and Regenerative Medicine, The University of Western Australia, Nedlands, WA, 6009, Australia

[h] Flinders Institute for Nanoscale Science & Technology, Flinders University, Bedford Park, SA 5042, Australia

[i] National Deuteration Facility, Australian Nuclear Science and Technology Organisation (ANSTO), New Illawarra Road, Lucas Heights, NSW 2234, Australia

* Corresponding author.

E-mail: nadim.darwish@curtin.edu.au

Water Contact Angle

Figure 2a–f show the water wettability of SAMs **S–1** and **S–2** before and after applying the electrochemical potential. Before applying any potentials, SAM **S–2** (Si–D) is slightly more hydrophilic than SAM **S–1** (Si–H). This can be explained by the ability of the deuterated surface in forming a slightly stronger hydrogen bonding with H_2O (for e.g. the boiling point of D_2O is 101.4 ˚C versus 100 ˚C for water). The change in the water contact angles as a function of the applied potential on SAM **S–2** is also slightly smaller than that on SAM **S–1**. For SAM **S–1**, the water contact angles changes from 82 ° ± 7 ° to 72 ° ± 4 ° and 55 ° ± 5 ° when the potential applied changed from + 0.6 V for 1 minute to + 1.5 V for 10 minutes. In comparison, the initial water contact for SAM **S–2** was 75 ° ± 9 ° and only diminished to 66 ° ± 7 ° and 57 ° ± 7 ° when 0.6 V and 1.5 V was applied, respectively. Similar trends were also observed at negative potentials. (Figure S1, Supporting Information)

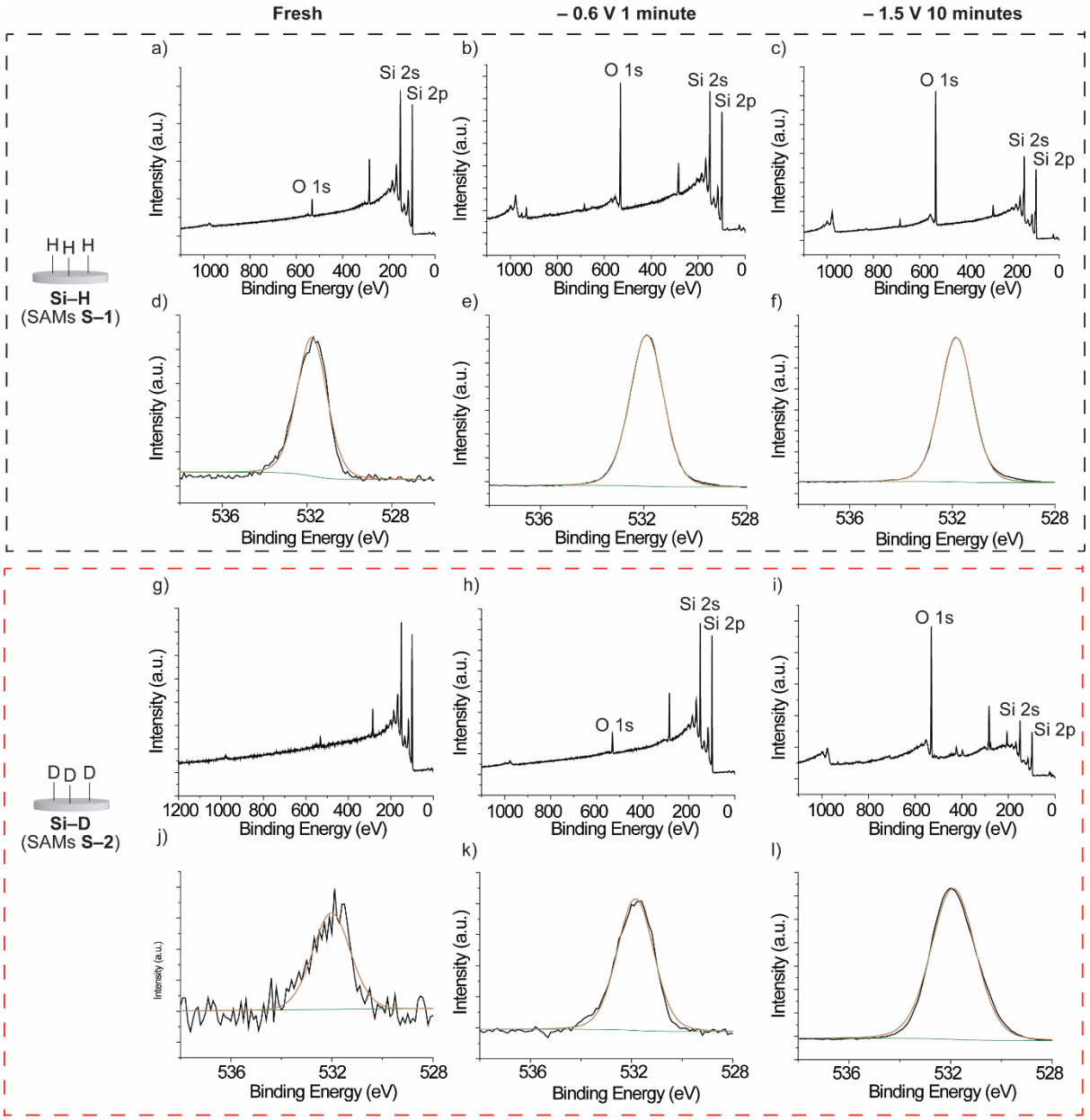

Figure S1. *XPS survey spectra of SAM **S–1** for (a) freshly prepared, (b) after oxidation at – 0.6 V, and (c)after oxidation at – 1.5 V. XPS high resolution O 1s spectra of SAM **S–1** for **(d)** freshly prepared, (e) after oxidation at – 0.6 V, and (f) after oxidation at – 1.5 V. XPS survey spectra of SAM **S–2** for (g) freshly prepared, (h) after oxidation at – 0.6 V, and (i) after oxidation at – 1.5 V. XPS high resolution O 1s spectra of SAM **S–2** for **(j)** freshly prepared, (k) after oxidation at – 0.6 V, and (l) after oxidation at – 1.5 V.*

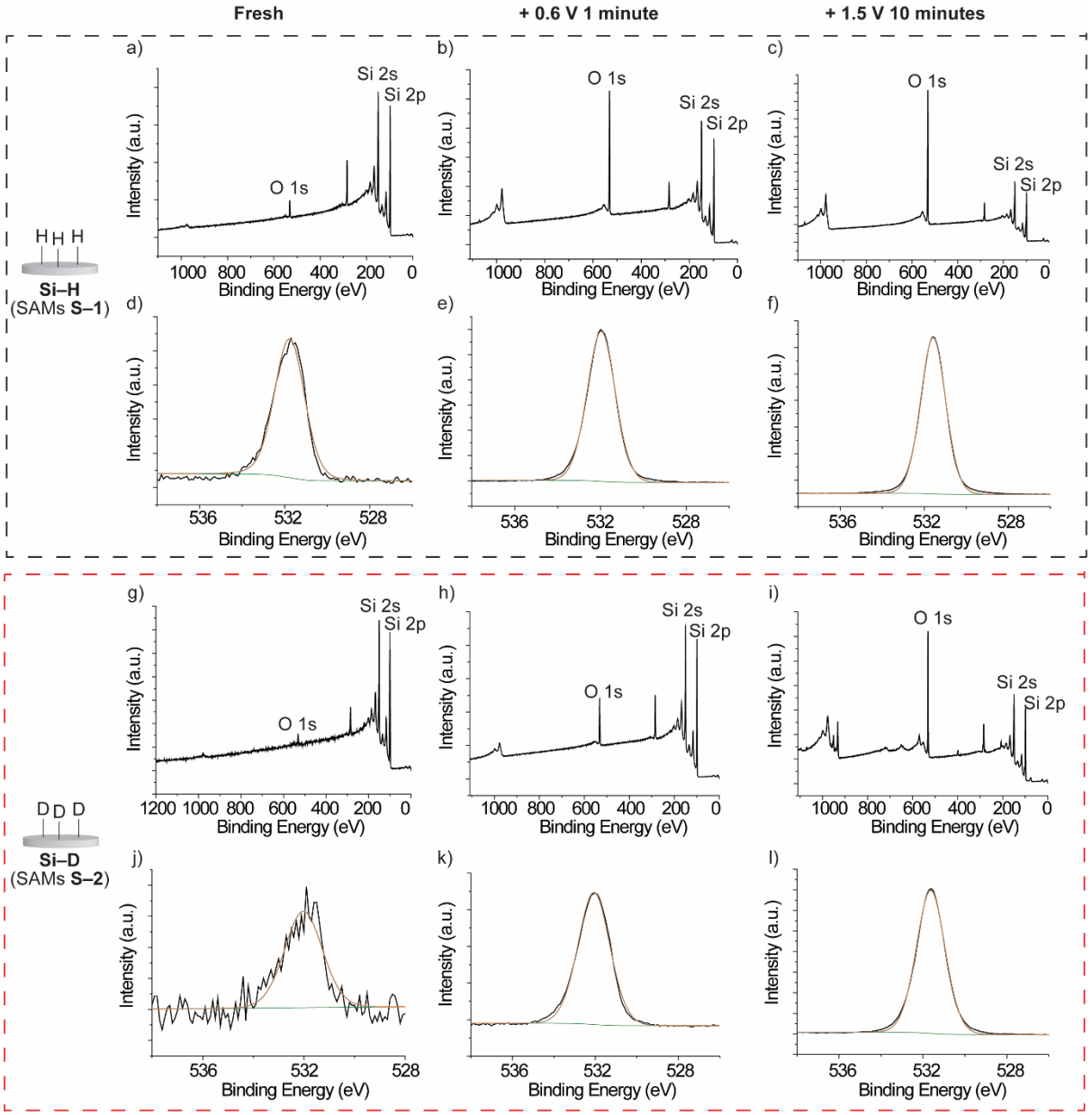

Figure S2. *XPS survey spectra of SAM **S–1** for (a) freshly prepared, (b) after oxidation at 0.6 V, and (c) after oxidation at 1.5 V. XPS high resolution O 1s spectra of SAM **S–1** for **(d)** freshly prepared, (e) after oxidation at 0.6 V, and (f) oxidized at 1.5 V. XPS survey spectra of SAM **S–2** for (g) freshly prepared, (h) after oxidation at 0.6 V, and (i) after oxidation at 1.5 V. XPS high resolution O 1s spectra of SAM **S–2** for **(j)** freshly prepared, (k) after oxidation at 0.6 V, and (l) after oxidation at 1.5 V.*

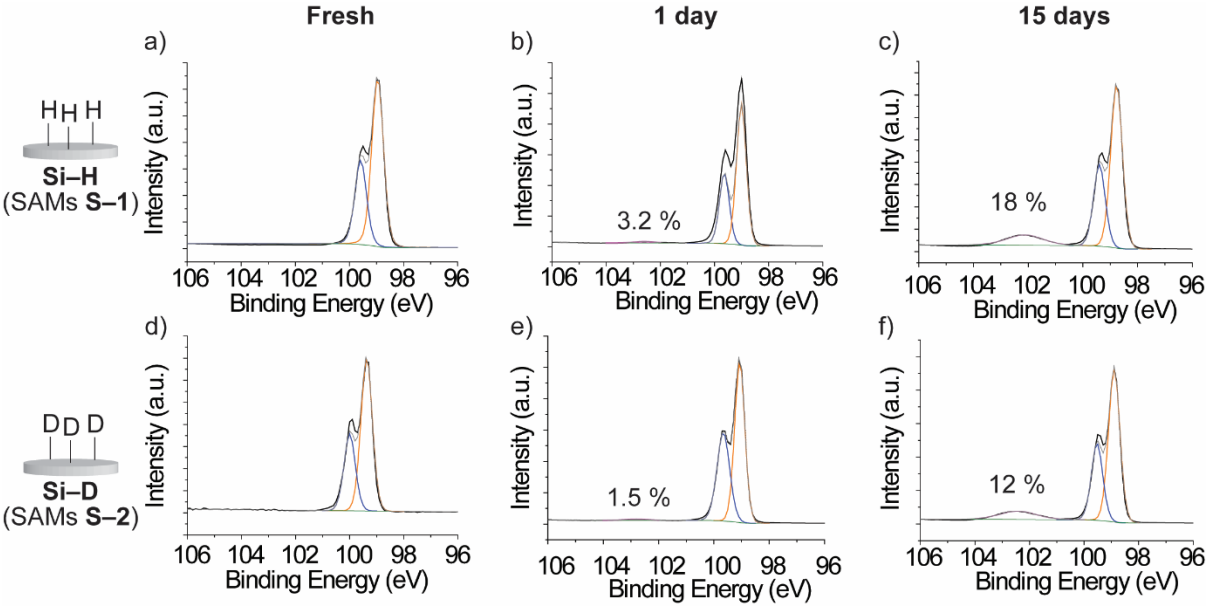

Figure S3*. XPS high resolution Si 2p spectra for SAMs* ***S–1*** *(a) freshly prepared, (b) after oxidation in ambient conditions (21 ℃ and 30% relative humidity) for 1 day, and (c) after oxidation in ambient conditions for 15 days. XPS high resolution Si 2p spectra for SAMs* ***S–2*** *(d) freshly prepared, (e) after oxidation in ambient conditions for 1 day, and (f) after oxidation in ambient conditions for 15 days.*

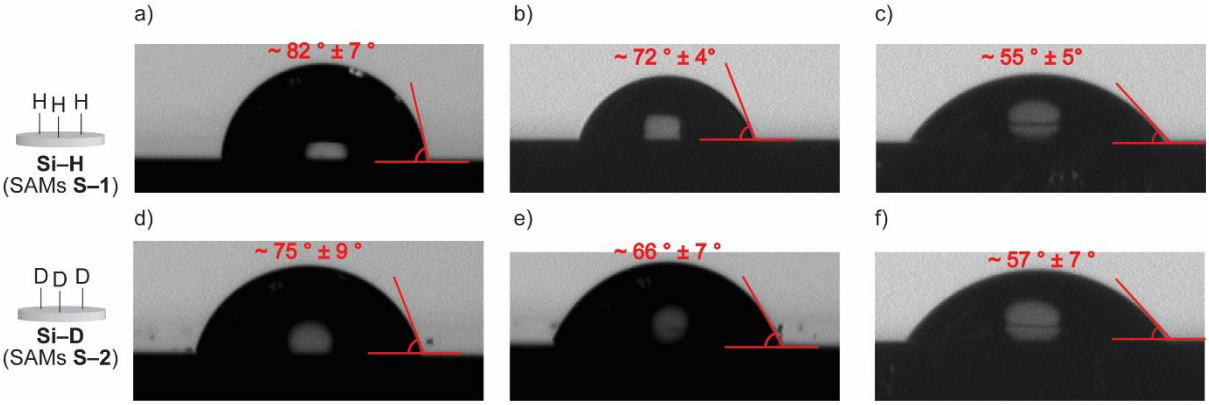

Figure S4. *The static image of a water droplet on SAM **S–1** a) freshly prepared, b) after an electrochemical potential of +0.6 V was applied for 1 minute, c) after an electrochemical potential of +1.5 V was applied for 10 minutes. The static image of a water droplet on SAM **S–2** d) freshly prepared, e) after an electrochemical potential of +0.6 V was applied for 1 minute, f) after an electrochemical potential of +1.5 V was applied for 10 minutes.*

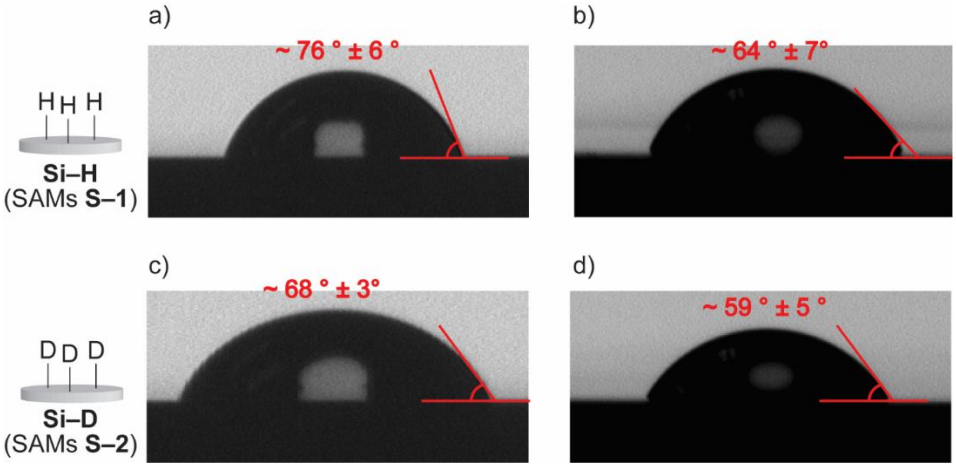

Figure S5. *The static image of a water droplet on SAM **S–1** a) after an electrochemical potential of – 0.6 V was applied for 1 minute, b) after an electrochemical potential of – 1.5 V was applied for 10 minutes. The static image of a water droplet on SAM **S–2** c) after an electrochemical potential of – 0.6 V was applied for 1 minute, d) after an electrochemical potential of – 1.5 V was applied for 10 minutes.*

Table S1. The percentage of SiO_x relative to Si surface from XPS results (%).

	Si–H	Si–D
Fresh	0	0
– 0.6 V 1 minute	20.7%	1.7%
– 1.5 V 10 minutes	43%	29.5%
+ 0.6 V 1 minute	16.2%	1.3%
+ 1.5 V 10 minutes	39.6%	22%

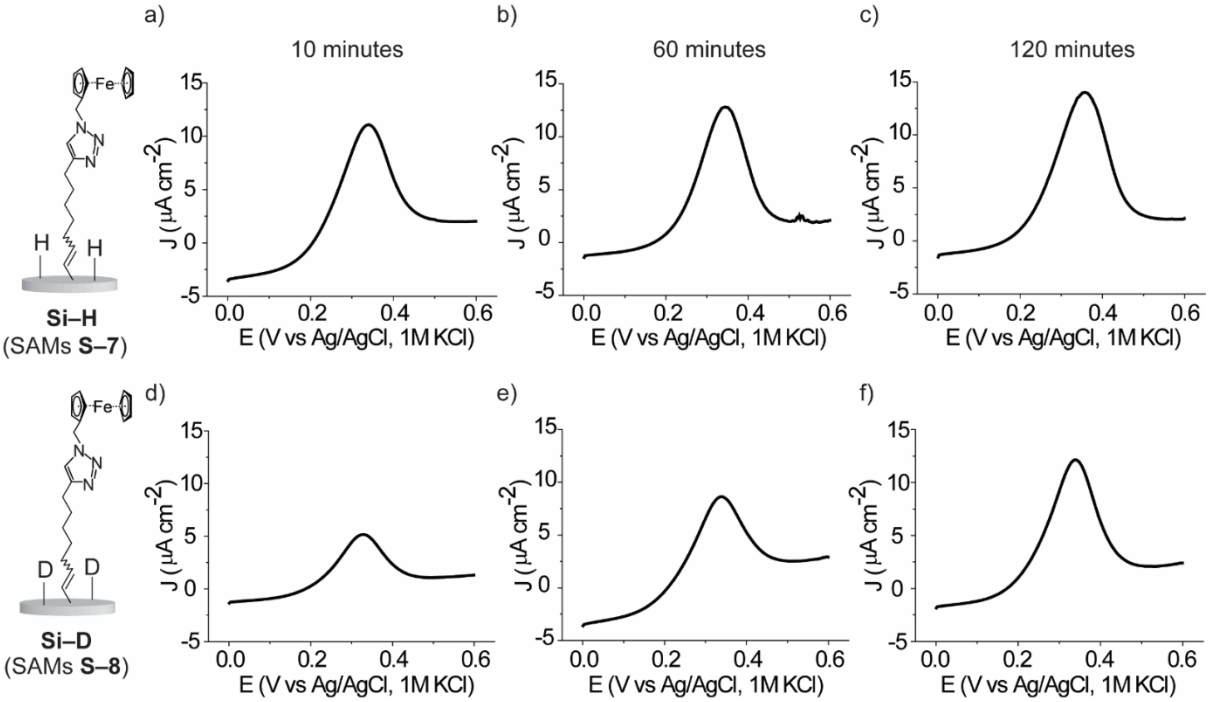

Figure S6. *Cyclic voltammetry for SAMs S–7 in which different hydrosilylation reaction times, with 1,8-nonadiyne under UV light, were applied, a) 10 minutes, b) 60 minutes, and c) 120 minutes. Cyclic voltammetry for SAMs S–8 in which different hydrosilylation reaction times, with 1,8-nonadiyne under UV light, were applied, d) 10 minutes, e) 60 minutes, and f) 120 minutes.*

Table S2. The corresponding surface coverages calculated from the oxidation waves of the CVs in Figure S6. The time corresponds to that used for the hydrosilylation reaction.

Surface / Time (minutes)	Si–H	Si–D
10	$(1.20 \pm 0.30) \times 10^{14}$	$(7.90 \pm 1.96) \times 10^{13}$
60	$(1.54 \pm 0.34) \times 10^{14}$	$(1.15 \pm 0.26) \times 10^{14}$
120	$(1.81 \pm 0.43) \times 10^{14}$	$(1.63 \pm 0.42) \times 10^{14}$

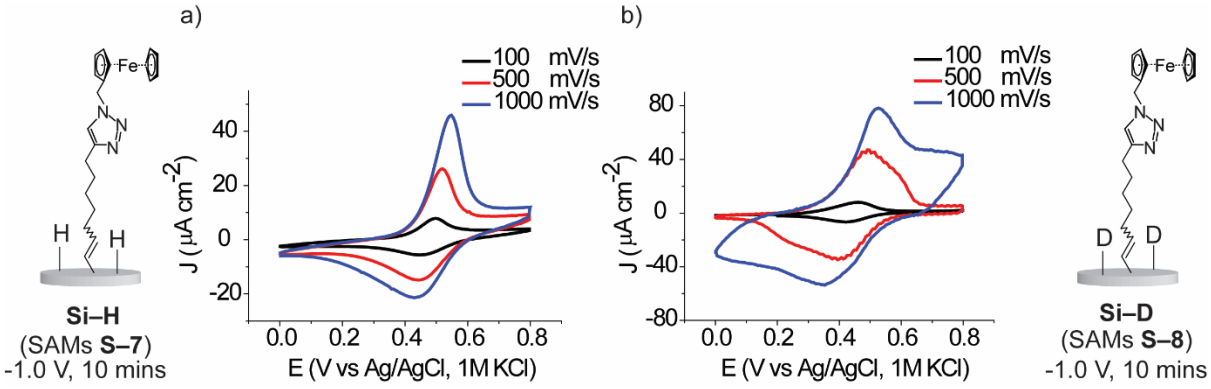

Figure S7. *a) Cyclic voltammetry for SAMs **S–7** which is obtained after applying to SAMs **S–5** an electrochemical potential of – 1.0 V for 10 minutes at different scan rates of 100 mV/s, 500 mV/s, and 1000 mV/s. b) Cyclic voltammetry for SAMs **S–8** which is obtained after applying to SAMs **S–6** an electrochemical potential of – 1.0 V for 10 minutes at different scan rates of 100 mV/s, 500 mV/s, and 1000 mV/s.*

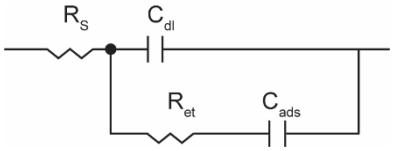

Figure S8. *The Randles circuit used to fit the EIS data. The k_{et} is calculated according to the following equations:*

$C_{dI} = \left(\frac{C}{A}\right)(A)$

$C_{ads} = \left(\frac{n2F2A\Gamma}{4RT}\right)$

$R_{ct} = \left(\frac{2RT}{n2F2A\Gamma Ket}\right)$

In the above equations, C_{dl} is the double layer capacitance, C/A is the double layer capacitance per unit area, A is the electrode area, Γ is the coverage of the electroactive species per unit area, C_{ads} is the adsorption pseudocapacitance. R_{et} is the charge-transfer resistance, n is the number of electrons transferred and the rate constant is determined by the following equation:

$k_{et} = \left(\frac{1}{2RetCads}\right)$

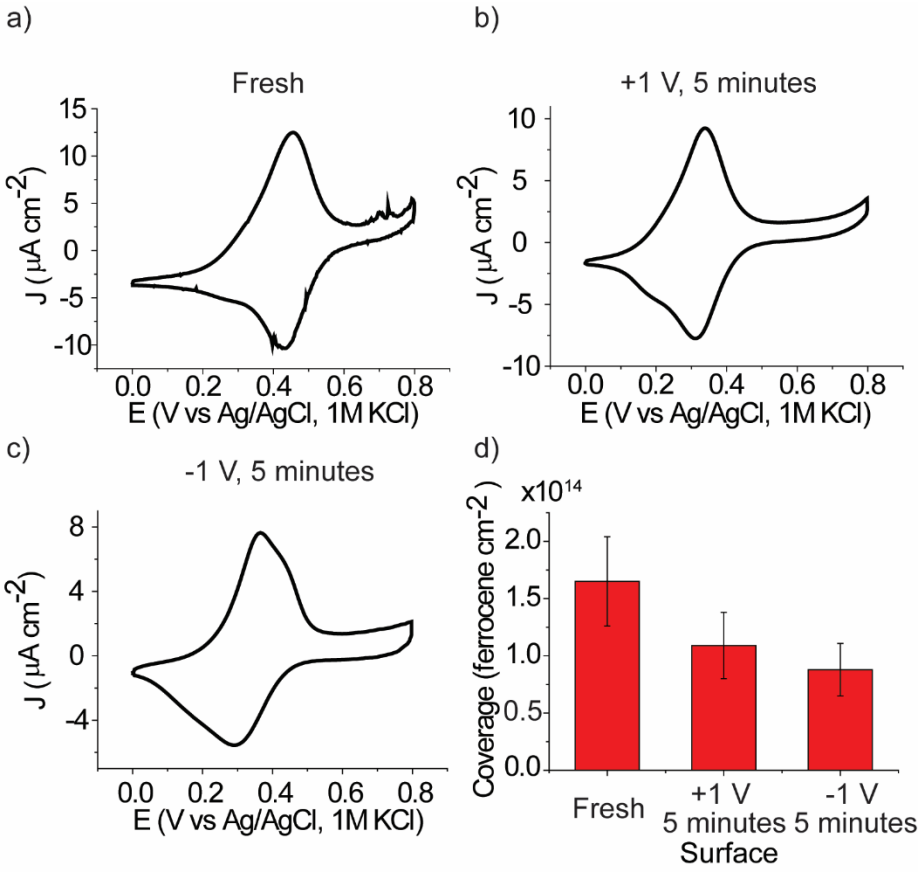

Figure S9. *Cyclic voltammetry for a) SAMs **S–8** which is fresh prepared, b) SAMs **S–8** which is obtained after applying to SAMs **S–6** an electrochemical potential of + 1.0 V for 5 minutes in a solution saturated by bubbled O_2 c) SAMs **S–8** which is obtained after applying to SAMs **S–6** an electrochemical potential of – 1.0 V for 5 minutes in a solution saturated by bubbled O2. d) The corresponding surface coverages calculated from the oxidation waves of the CVs in (a), (b), and (c). The error bars in (d) are the standard deviation of surface coverages from the mean value of three different surfaces. All CVs data were performed at the scan rate of 0.1 V/s.*

Table S3. The value of best fits to the original EIS data presented in fresh state of SAMs **S–7** and **S–8**. The EIS data were interpreted by curve fitting the data to Randles circuit.

Type	$\mathbf{R_{sol}}$ **(Ω)**	$\mathbf{C_{dl}}$ **(F)**	$\mathbf{R_{et}}$ **(Ω)**	$\mathbf{C_{ads}}$ **(F)**	$\boldsymbol{k}_{\mathbf{et}}$ **(s^{-1})**
Si–D Fresh	1.57 ± 0.18	$(1.42 \pm 0.09)\times10^{-6}$	526.7 ± 8.36	$(4.44 \pm 0.09)\times10^{-5}$	21.37 ± 0.74
Si–H Fresh	7.25 ± 0.11	$(9.17 \pm 1.54)\times10^{-6}$	36.59 ± 1.23	$(8.00 \pm 0.17)\times10^{-5}$	170.76 ± 8.94

Table S4. The value of best fits to the original EIS data presented in Figure 4a. The EIS data were interpreted by curve fitting the data to Randles circuit.

Time (minut	R_{sol} (Ω)	C_{dl} (F)	R_{et} (Ω)	C_{ads} (F)	k_{et} (s^{-1})
1	9.22 ± 0.44	$(4.62 \pm 0.69)\times10^{-6}$	78.45 ± 4.26	$(5.10 \pm 0.26)\times10^{-5}$	124.97 ± 12.19
5	12.45 ± 0.14	$(3.75 \pm 0.74)\times10^{-6}$	79.37 ± 1.65	$(6.12 \pm 0.17)\times10^{-5}$	102.93 ± 4.82
10	6.87 ± 0.19	$(3.58 \pm 0.34)\times10^{-6}$	91.24 ± 2.56	$(6.95 \pm 0.12)\times10^{-5}$	78.35 ± 3.45

Table S5. The value of best fits to the original EIS data presented in Figure 4b. The EIS data were interpreted by curve fitting the data to Randles circuit.

Time (minute)	R_{sol} (Ω)	C_{dl} (F)	R_{et} (Ω)	C_{ads} (F)	k_{et} (s^{-1})
1	8.46 ± 0.25	$(1.71 \pm 0.40)\times10^{-6}$	53.7 ± 3.21	$(8.03 \pm 0.21)\times10^{-5}$	115.95 ± 9.33
5	7.53 ± 0.22	$(1.63 \pm 0.41)\times10^{-6}$	91.38 ± 2.48	$(6.06 \pm 0.23)\times10^{-5}$	90.29 ± 5.60
10	4.32 ± 0.24	$(1.66 \pm 0.32)\times10^{-6}$	152.3 ± 4.4	$(6.67 \pm 0.36)\times10^{-5}$	49.22 ± 3.83

Table S6. The value of best fits to the original EIS data presented in Figure 4c. The EIS data were interpreted by curve fitting the data to Randles circuit.

Time (minute)	R_{sol} (Ω)	C_{dl} (F)	R_{et} (Ω)	C_{ads} (F)	k_{et} (s^{-1})
1	6.84 ± 0.17	(1.13 ± 0.18)×10^{-6}	59.23 ± 1.35	(7.94 ± 0.13)×10^{-5}	106.32 ± 4.05
5	6.37 ± 0.13	(1.26 ± 0.23)×10^{-6}	79.43 ± 2.39	(7.36 ± 0.12)×10^{-5}	85.53 ± 3.83
10	8.49 ± 0.09	(1.47 ± 0.15)×10^{-6}	232.38 ± 2.47	(6.03 ± 0.05)×10^{-5}	35.68 ± 0.66

Table S7. The value of best fits to the original EIS data presented in Figure 4e. The EIS data were interpreted by curve fitting the data to Randles circuit.

Time (minute)	R_{sol} (Ω)	C_{dl} (F)	R_{et} (Ω)	C_{ads} (F)	k_{et} (s^{-1})
1	3.25 ± 0.13	(1.25 ± 0.03)×10^{-6}	672.9 ± 4.88	(4.53 ± 0.06)×10^{-5}	17.43 ± 0.64
5	11.79 ± 0.43	(2.25 ± 0.12)×10^{-6}	656.2 ± 7.68	(5.48 ± 0.07)×10^{-5}	16.79 ± 0.68
10	3.26 ± 0.08	(1.77 ± 0.06)×10^{-6}	619.3 ± 5.95	(6.25 ± 0.06)×10^{-5}	16.06 ± 0.40

Table S8. The value of best fits to the original EIS data presented in Figure 4f. The EIS data were interpreted by curve fitting the data to Randles circuit.

Time (minute)	R_{sol} (Ω)	C_{dl} (F)	R_{et} (Ω)	C_{ads} (F)	k_{et} (s^{-1})
1	1.94 ± 0.11	(4.35 ± 0.32)×10^{-7}	547.6 ± 10.08	(5.24 ± 0.10)×10^{-5}	16.40 ± 0.33
5	32.09 ± 0.95	(7.39 ± 0.88)×10^{-7}	422.8 ± 8.36	(7.08 ± 0.12)×10^{-5}	13.90 ± 0.33
10	1.99 ± 0.08	(5.44 ± 0.31)×10^{-7}	385.7 ± 4.71	(8.07 ± 0.11)×10^{-5}	12.92 ± 0.25

Table S9. The value of best fits to the original EIS data presented in Figure 4g. The EIS data were interpreted by curve fitting the data to Randles circuit.

Time (minute)	R_{sol} (Ω)	C_{dl} (F)	R_{et} (Ω)	C_{ads} (F)	k_{et} (s^{-1})
1	2.03 ± 0.07	$(9.37 \pm 0.33)\times10^{-7}$	522.9 ± 4.34	$(6.75 \pm 0.06)\times10^{-5}$	14.17 ± 0.24
5	2.04 ± 0.08	$(4.85 \pm 0.28)\times10^{-7}$	348.8 ± 6.94	$(1.15 \pm 0.04)\times10^{-4}$	12.47 ± 0.66
10	1.97 ± 0.08	$(5.38 \pm 0.30)\times10^{-7}$	461.7 ± 8.33	$(1.22 \pm 0.04)\times10^{-4}$	8.88 ± 0.44

Table S10. The value of best fits to the original EIS data presented in Figure 4i. The EIS data were interpreted by curve fitting the data to Randles circuit.

Time (minute)	R_{sol} (Ω)	C_{dl} (F)	R_{et} (Ω)	C_{ads} (F)	k_{et} (s^{-1})
1	8.74 ± 0.25	(1.34 ± 0.08)×10^{-6}	39.56 ± 0.53	(9.54 ± 0.12)×10^{-5}	132.48 ± 3.37
5	8.76 ± 0.22	(1.45 ± 0.21)×10^{-6}	75.28 ± 0.88	(8.96 ± 0.23)×10^{-5}	74.13 ± 2.69
10	15.89 ± 0.56	(8.74 ± 0.89)×10^{-6}	102.9 ± 6.71	(9.96 ± 0.21)×10^{-5}	48.79 ± 3.94

Table S11. The value of best fits to the original EIS data presented in Figure 4j. The EIS data were interpreted by curve fitting the data to Randles circuit.

Time (minute)	R_{sol} (Ω)	C_{dl} (F)	R_{et} (Ω)	C_{ads} (F)	k_{et} (s^{-1})
1	7.12 ± 0.35	(1.54 ± 0.13)×10^{-6}	258.46 ± 9.73	(5.11 ± 0.08)×10^{-5}	37.86 ± 1.94
5	10.42 ± 0.19	(1.77 ± 0.15)×10^{-6}	419.46 ± 6.82	(8.21 ± 0.14)×10^{-5}	14.52 ± 0.47
10	21.85 ± 0.44	(1.74 ± 0.08)×10^{-6}	526 ± 8.28	(8.61 ± 0.17)×10^{-5}	11.04 ± 0.38

Table S12. The value of best fits to the original EIS data presented in Figure 4k. The EIS data were interpreted by curve fitting the data to Randles circuit.

Time (minute)	R_{sol} (Ω)	C_{dl} (F)	R_{et} (Ω)	C_{ads} (F)	k_{et} (s^{-1})
1	15.26 ± 0.45	(3.10 ± 0.26)×10^{-6}	1582 ± 40.38	(6.94 ± 0.09)×10^{-5}	4.55 ± 0.17
5	23.44 ± 0.32	(1.35 ± 0.20)×10^{-6}	1692 ± 105	(8.43 ± 0.49)×10^{-5}	3.51 ± 0.39
10	17.46 ± 0.93	(1.46 ± 0.16)×10^{-6}	2976 ± 126	(6.96 ± 0.56)×10^{-5}	2.41 ± 0.27

Table S13. The value of best fits to the original EIS data presented in Figure 4m. The EIS data were interpreted by curve fitting the data to Randles circuit.

Time (minute)	R_{sol} (Ω)	C_{dl} (F)	R_{et} (Ω)	C_{ads} (F)	k_{et} (s^{-1})
1	157.7 ± 3.24	$(2.97 \pm 0.23)\times10^{-6}$	1289 ± 28.44	$(2.28 \pm 0.04)\times10^{-5}$	17.01 ± 0.65
5	2.33 ± 0.11	$(1.49 \pm 0.05)\times10^{-6}$	1479 ± 20.53	$(3.38 \pm 0.07)\times10^{-5}$	10.00 ± 0.34
10	1456 ± 28	$(8.07 \pm 1.68)\times10^{-6}$	1776 ± 82.6	$(3.47 \pm 0.11)\times10^{-5}$	8.11 ± 0.60

Table S14. The value of best fits to the original EIS data presented in Figure 4n. The EIS data were interpreted by curve fitting the data to Randles circuit.

Time (minute)	R_{sol} (Ω)	C_{dl} (F)	R_{et} (Ω)	C_{ads} (F)	k_{et} (s^{-1})
1	1303 ± 49.31	$(1.05 \pm 0.38)\times10^{-5}$	2438 ± 327.52	$(3.89 \pm 0.32)\times10^{-5}$	5.27 ± 0.98
5	20.4 ± 1.01	$(2.57 \pm 0.14)\times10^{-6}$	3840 ± 115.9	$(7.01 \pm 0.16)\times10^{-5}$	1.86 ± 0.10
10	$(8.85 \pm 0.3)\times10^{-4}$	$(1.48 \pm 0.15)\times10^{-6}$	7372 ± 270.97	$(4.87 \pm 0.16)\times10^{-5}$	1.39 ± 0.09

.

Table S15. The value of best fits to the original EIS data presented in Figure 4o. The EIS data were interpreted by curve fitting the data to Randles circuit.

Time (minute)	R_{sol} (Ω)	C_{dl} (F)	R_{et} (Ω)	C_{ads} (F)	k_{et} (s^{-1})
1	448 ± 54.03	$(2.02 \pm 0.36)\times10^{-5}$	11628 ± 325.36	$(1.60 \pm 0.03)\times10^{-5}$	2.69 ± 0.12
5	232.7 ± 18.74	$(3.73 \pm 0.04)\times10^{-6}$	14880 ± 235.26	$(2.56 \pm 0.10)\times10^{-5}$	1.31 ± 0.07
10	525.9 ± 31.83	$(2.20 \pm 0.04)\times10^{-6}$	28976 ± 877.97	$(1.65 \pm 0.08)\times10^{-5}$	1.05 ± 0.07